Journal of
Geography & Natural Disasters

Ali and Mohammed, J Geogr Nat Disast 2016, S6
DOI: 10.4172/2167-0587.S6-002

Research Article Open Access

Impact of Industrial Activities on Land Surface Temperature Using Remote Sensing and GIS Techniques - A Case Study in Jubail, Saudi Arabia

Abdelnasser Rashash Ali* and El-Shirbeny Mohammed

National Authority for Remote Sensing and Space Sciences (NARSS), Saudi Arabia

Abstract

Land Surface temperature (LST) is one of the most important variables for determining the state within the climate system. Thermal infrared (TIR) remote sensing used to monitor air temperature and affecting microclimate in urban areas. TIR remote sensing techniques have been applied for analyzing LST patterns and its relationship with surface characteristics, assessing urban heat island (UHI), and relating LST with surface energy fluxes to characterize landscape properties and processes. In the present study, a remote sensing was combined with a geographic information system (GIS) environment for determine the impact of industrial areas on Surface Temperature using of TIR Remote Sensing through Landsat ETM+ data (band 6.1) and comparing the relationships between urban surface temperature and land cover types in Jubail City in Saudi Arabia. The study showed the increase of urban surface temperature near the industrial area in comparison with suburban areas. The center of the heat island was concentrated above the industrial area and its adjacent urban areas. Iron and steel factories raise the temperature to 80°C which affects air temperature of nearby areas. This effect may extend to the buffer zone area ranging from 500-2000 m.

Keywords: Surface temperature; Thermal Infrared; Heat island; Industrial area; NDVI and UHI

Introduction

Land Surface temperature is one of the most important variables for determining the state of the climate system. It is the source of change in air surface temperature and climate system related. The LST has a direct impact on air temperature, and it is also one of the key parameters in the physics of land surface processes [1]. Since then, with recent progress in remote sensing and satellite thermal data acquired at daytime have been widely used to detect surface UHIs on meso or large scales when heat island intensities are greatest [2]. The Urban Heat Island (UHI) is the important phenomenon in urban geographic studies, which traps heat in thermal mass like asphalt, concrete, bricks, stones and roads, which absorb, store and then re-emit this heat to the urban air at night [3], the urban temperatures are 2-5 higher than those in a rural surroundings [4]. It is a key variable for the detection of climate change and assessing the relative importance of anthropogenic and natural influences. It is a prime driver of many impacts of natural and human created systems. The urbanization and industrialization are a main factor for island heat.

Setturu [5] and Weng [6] applied the TIR remote sensing techniques in urban climate and environmental studies; for analyzing LST patterns and its relationship with surface characteristics, assessing urban heat island to characterize landscape properties, processes and patterns.

The climatic elements are almost observed by climate stations in cities, almost each city content one station, and it doesn't express actual microclimate conditions in many cases.

The city under investigation doesn't have climate station, the thermal remote sensing is important because it can cover greater areas to providing more details, remotely sensed TIR data are unique sources of information to define surface heat islands [6].

LST and emissivity data are used in urban climate and environmental studies, mainly for analyzing LST patterns and its relationship with surface characteristics, for assessing urban heat island, and for relating LSTs with surface energy fluxes in order to characterize landscape properties, patterns, and processes [7].

Thermal remote sensing has been used in many studies to retrieve LST and assess the urban heat island and climatic conditions [7-11]. Despite the numerous studies conducted on this issue, no study provided the impact of industrial areas in urban.

To estimate the thermal condition of land surface by satellite image, it is necessary to find the relationship between the surface temperature, surrounding topography and land cover/use. To estimate LST from satellite thermal data, the digital number (DN) of image pixels needs to be converted into spectral radiance using the sensor calibration data.

Landsat ETM+ with 60 m, spatial resolution of the thermal infrared band enables experts to define the more detailed surface temperature [6]. This research aims to evaluate the use of Landsat ETM+ data for identifying temperature differences in urban areas, to analyze and compare the relationship between urban surface temperature and land cover types, and to estimate the impact of industrial areas upon adjacent area.

Specific objectives of this research are investigated the relationships between industrial areas and LST in Jubail City and comparing the relationships between urban surface temperature and land cover types using remote sensing and GIS.

Study Area

Location of study area

The investigated area lies on the north-eastern coast the of Arabian

***Corresponding author:** Dr. Abdelnasser Rashash Ali, Mail: 23 Joseph Tito Street, El-Nozha El-Gedida, P.O. Box: 1564 Alf Maskan, Saudi Arabia, Tel: 201120594946, +2047 3300179; E-mail: rahash.gis@gmail.com

Received September 19, 2016; **Accepted** October 31, 2016; **Published** November 04, 2016

Citation: Ali AR, Mohammed ES (2016) Impact of Industrial Activities on Land Surface Temperature Using Remote Sensing and GIS Techniques - A Case Study in Jubail, Saudi Arabia. J Geogr Nat Disast S6: 002 doi: 10.4172/2167-0587.S6-002

peninsula it is bounded by latitude: 27 10 00 to 26 25 N, and longitude: 49 50 00 to 49 30 00 E on the coast of Arabian golf, it represents the desert area with extremely high temperature in summer (Figure 1).

In 1977, Jubail, on Saudi Arabia's Gulf Coast, was a small fishing community of sum of 8,000 inhabitants. Today, it contains the largest civil engineering projects in the world.

During the last decade, Jubail City became the biggest industrial area.

Nowadays, Arabian Gulf is represented by the major part of Jubail City and some surrounding areas, which is reported to have rapid built-up expansion since the last decade resulted in air pollution and greenhouse gas emission problems that seriously impact the human health [12].

Climatic condition

The climate in Jubail City is hyper-arid, dry desert with great temperature extremes. In February, the average maximum temperatures are 31.7°C and average minimum 4.5°C, while in July the average maximum is 48.7°C and minimum is 29°C. The wettest month is January with an average of 41.4 mm of precipitation while the driest month is summer season with 0.0 mm falling, The Jubail area characterized by instability in the rain amount that fall in the same month (Table 1).

Methodology and Data

Data were obtained by the Landsat 7 Enhanced Thematic Mapper Plus (ETM+) sensors. That acquire thermal temperature data and store information as a digital number (DN) thermal band (band 6.1 and 6.2 in ETM+) The Landsat images were rectified to the UTM projection system (datum WGS84, zone 36), and it is possible to convert these DNs to degrees Kelvin using two processes.

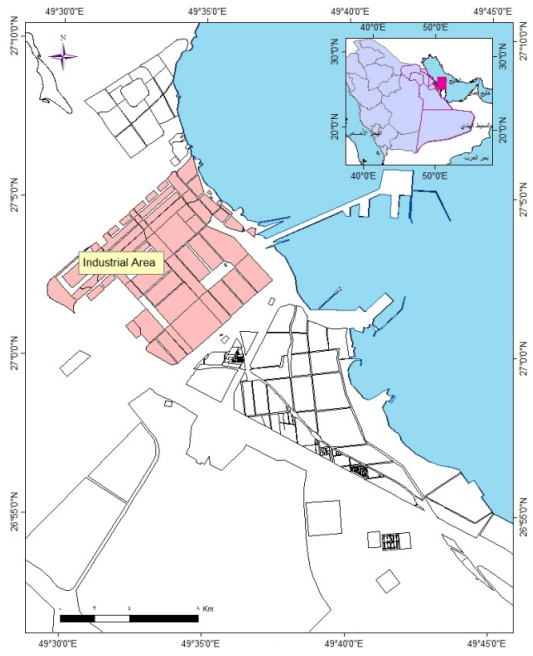

Figure 1: Map of the study area (Jubail City, KSA).

Radiances are in units of W/(m^2 *sr*μm) and the transmission and emissivity are unit less. The radiances in TM band 6 (high gain on ETM+) were calculated from digital numbers (DN) using standard NASA equations to correct for gain and offset at the detector [13,14]. In ETM+, band 6 captures the radiant thermal energy between 10.4 and 12.5 Am, at the atmospheric window between O_3 and CO_2 atmospheric absorptions.

Preprocessing remote sensing

The Landsat7 Enhanced Thematic Mapper Plus (ETM+) sensor record bands of spectral data in the visible, infrared, and thermal portions of the electromagnetic spectrum and The spatial resolution of this sensor is 30 m, except thermal band of 60 m resolution (USGS., 2001). Landsat data from Landsat-7 image was obtained (Path 164/Row 41), acquired on 18 May, 2001 images were analyzed. The Landsat images were rectified to the UTM projection system (Ain el abed datum and zone 39N).

The following procedures in Figure 2 were carried out to derive the digital surface temperature, generate the temperature color map, analyze the data, create buffer around the urban heat island and Produce spectral profile land cover, Landsat ETM+ was used effectively to identify the spatial distribution characteristics of surface temperature and land use/land cover classes.

The image had good weather conditions without or with little clouds in the study area. Atmospheric corrections processed using ENVI Flash tools [15]. The band ETM+ 6.1 were analyzed to extract LST. Whereas the bands 4, 3, 2 were used for Supervised NDVI and the bands 7, 4, 2 were used for the color representation study area.

The Post processing

The first process is to convert the DNs to radiance values using the bias and gain values specific to the individual pixel. The second process is to convert the radiance data to degrees in Kelvin [15,16]. The third one is to convert the temperature in Kelvin to the temperature Celsius.

Conversion the Digital Number (DN) to Spectral Radiance (Lλ): Radiance (W/m^2* Sr * μm) in TM band 6.1 (high gain on ETM+) were calculated from digital numbers (DN) using standard NASA equations to correct gain and offset at the detector. In TM and ETM+, band 6 captures the radiant thermal energy between 10.4 and 12.5 Am, at the atmospheric window between O_3 and CO_2 atmospheric absorptions [17].

The spectral radiance (Lλ) it was calculated using the following equation [17]:

$$L\lambda = ((LMAX\lambda - LMIN\lambda)/(QCALMAX-QCALMIN)) * (DN-QCALMIN) + LMIN\lambda$$

Where,

	Jan	Feb	Mar	Apr	May	Jun	Jul	Aug	Sep	Oct	Nov	Dec
Avg. Temperature °C	15.8	15.9	19.9	28.5	32.4	35	37.7	36.7	32.7	27.9	21.3	17.8
Max. Temperature °C	28.3	31.7	38.6	37.7	45.4	46.8	48.7	47.5	45.3	41.9	35.6	23.8
Min. Temperature °C	10	8	9.8	14.5	28.4	24.9	27.9	25.8	20.7	18.8	9.3	4.5
Avg. Rain Fall (mm)	41.4	0.7	0.3	3.7	0	0	0	0	0	0	0	0

Table 1: Average of climate elements (1961-2010) [13].

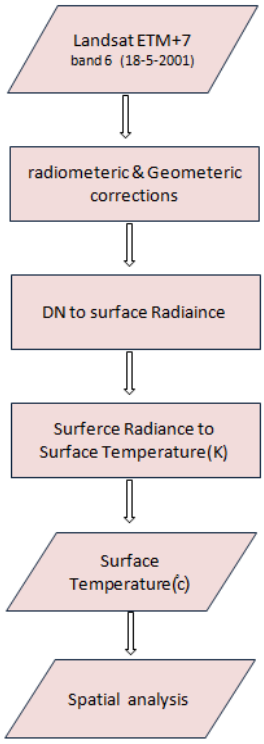

Figure 2: Flowchart showing the major steps of research procedures.

Lλ =Spectral radiance at the sensor's aperture (W/m-2* Sr-1 * μm)

DN = Quantized calibrated pixel value (Qcal)

QCALMIN = Minimum quantized calibrated pixel value corresponding to LMINλ [DN] = 1

QCALMAX = Maximum quantized calibrated pixel value corresponding to LMAXλ [DN] = 255

LMIN= Spectral at-sensor radiance that is scaled to Qcalmin (W/m-2* Sr-1 * μm)

LMAX = Spectral at-sensor radiance that is scaled to Qcalmax (W/m-2* Sr-1 * μm).

Conversion the spectral radiance to temperature in Kelvin: The ETM+ thermal band data could be converted from spectral radiance (as described above) to a more physically useful variable. These are the effectiveness at-satellite temperatures of the viewed Earth-atmosphere system under an assumption of unity emissivity and using pre-launch calibration constants [17,18].

Processing of the thermal band: Landsat 7 produces two thermal images; one acquired using a low gain setting (often referred to as band 6L), and the other using a high-gain setting (often referred to as band 6H). Band 6H is used in the Multi-Resolution Land Characteristics (MRLC) 2001 database because it is more sensitive to most land targets, especially vegetated targets. The thermal band is first converted from DN to at-satellite radiance and then to effective at-satellite temperature (T), Assuming surface emissivity = 1 [17] to convert radiance to temperature was used as the following equation [16,17]:

$$T = K2/(\ln (K1/L\lambda + 1))$$

Where, T = Top of the-atmosphere (ToA) in Kelvin, K1= Calibration constant = 666.09, W/(m2* sr * μm), K2 = Calibration constant = 1282.71 (Kelvin), ln = log Lλ = Spectral radiance in watts/(meter squared * sr * μm) [16,17] According to Barsi (2005) [18], with the atmospheric correction, the final surface temperatures have uncertainties less than 2 K when the atmosphere is relatively clear.

Conversion the Temperature unit From Kelvin to the Temperature "Celsius": The temperature in Celsius was calculated as the following equation:

$$T(C) = T - 273.13$$

Where: T (C) = Temperature "Celsius," T = Temperature "Kelvin", 273.13 = Zero Temperature "Kelvin".

Normalized difference vegetation index (NDVI)

Analyzing vegetation using remotely sensed data requires knowledge of the structure and function of vegetation and its reflectance the ratio of radiant energy reflected by a body to the energy incident on it, usually denoted as a percentage. Properties, Vegetation reflectance properties are used to derive vegetation indices to analyze various ecologies [15]. NDVI was used to transform multispectral data into a single image band representing vegetation distribution. The NDVI values indicate the amount of green vegetation present in the pixel; NDVI is calculated from the visible and near-infrared light reflected by vegetation [16,19,20]. NDVI maps were derived from ETM+ images as follows equation using the ENVI 5.1 software:

$$NDVI = ((IR - R)/(IR + R))$$

Where; NIR and Red are the spectral reflectance's in the ETM+ red and near-infrared bands, Calculations of NDVI for a given pixel always valid results fall between ranges from -1 to +1; where positive values indicate more green vegetation and negative values signify non-vegetated surface features.

Results and Discussions

The Landsat 7 ETM+ was acquired on 18 May, 2001, Band combination of 7, 4, 2 was used to give maximum information of land cover/use relevant to the investigated area, i.e. industrial zone, residential area of inner city with high density and its expansion, gardens, sand and water.

The thermal energy of different landforms showed greater variation in surface temperature of different surface patterns. Land surface temperature was extracted from thermal band 6.1 of Landsat 7 ETM+ (Figures 3 and 4). Analyses indicated that, the industrial, residential areas represent the highest surface temperature meanwhile vegetation and water bodies exhibit the lowest one.

Figure 5 shows the classification of surface temperature, where Factory chimneys site with dark-red color (from 60°C to 80°C) and Industrial zones with red colour (from 50°C to 60°C), Aluminum roofs material plus the thermal energy resulted from production activities that due to exhibited the highest temperature.

It is noticed that, factories could be considered the main source of heat in the Jubail industrial area as well as buildings. Those two elements are responsible for raising the surface temperature at urban area, rather than the development area and gardens.

The cooler areas that have temperature in the range of 37°C to 42°C (green and cyan color) are those supported by vegetation. This is the result of dissipating solar energy by absorbing surrounding

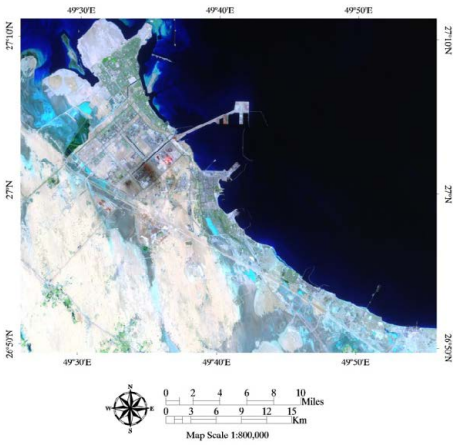

Figure 3: Band combination of channel 7, 4 and 2 of ETM+ in 2001.

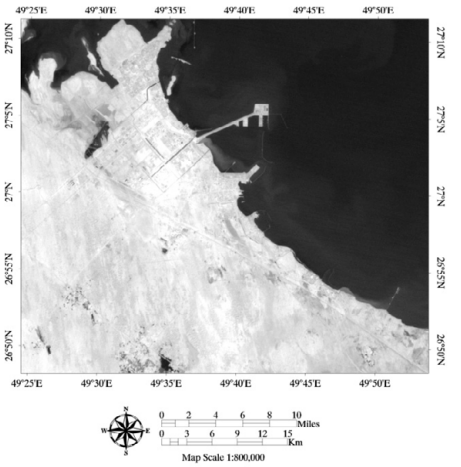

Figure: 4 Thermal bands (6.1) of Landsat 7 ETM+ of Jubail city.

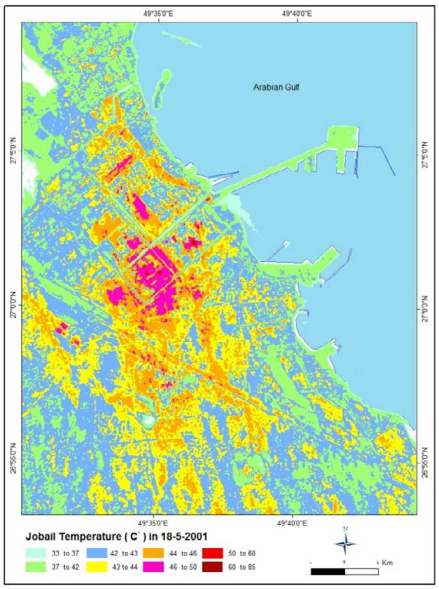

Figure 5: Surface temperature distribution of the study area.

heat and evaporation process from the leaves as well. The relationship and correlation between surface temperature and land cover types is elaborated, as shown in Figure 6.

Relationships between LST and land cover types

The vegetation in urban areas increases the amount of cooling by evapotranspiration because evapotranspiration reduces the temperature in the area around vegetation by converting solar radiation to latent heat, the cooling effect of green areas in Jubail has been confirmed as shown in Figures 5-8.

Whereas the relationship between LST and NDVI suffers from evident seasonal changes and it is better restricted to analysis of UHI effects during summer and early autumn.

Thermal cross section shows the difference between iron and steel factory and adjacent areas (Figure 9). The temperature in the perimeter of the chimney of iron factories rises to 80°C, affecting the temperature of nearby areas (Figure 9). This effect may extend into the distance between 500-2000 meters that could be considered as a buffer zone (Figure 10).

Land surface temperature changes between the different land cover, the location of verification point of LST recorded not cover water area

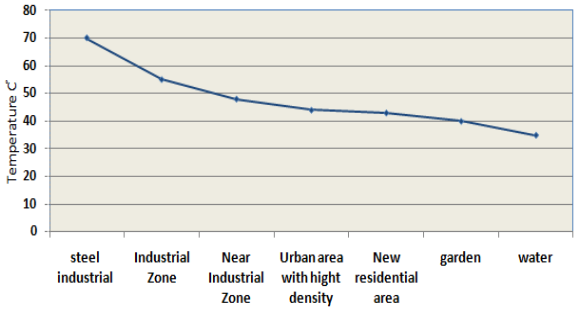

Figure 6: Thermal signature of land covers types in Jubail.

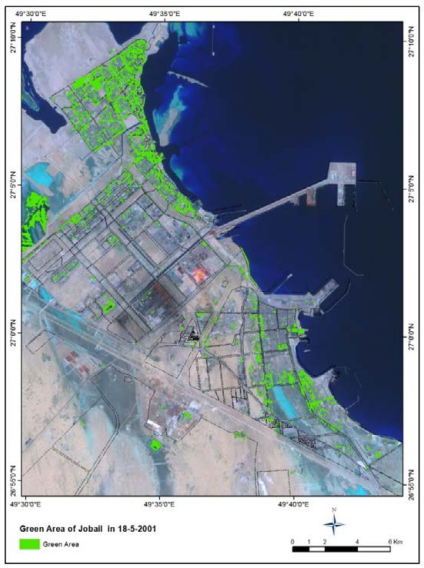

Figure 7: Surface temperature distribution of the study area.

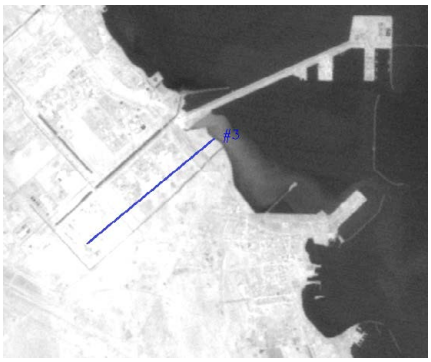

Figure 8: Thermal cross section.

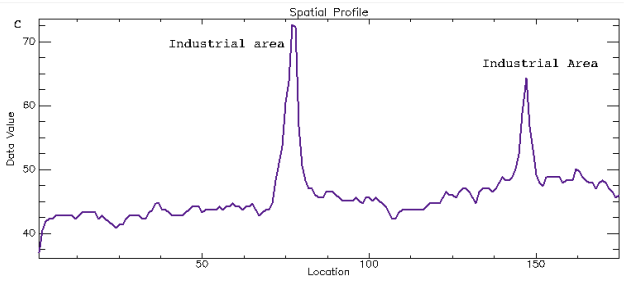

Figure 9: Thermal profile based on Figure 8 Thermal cross section.

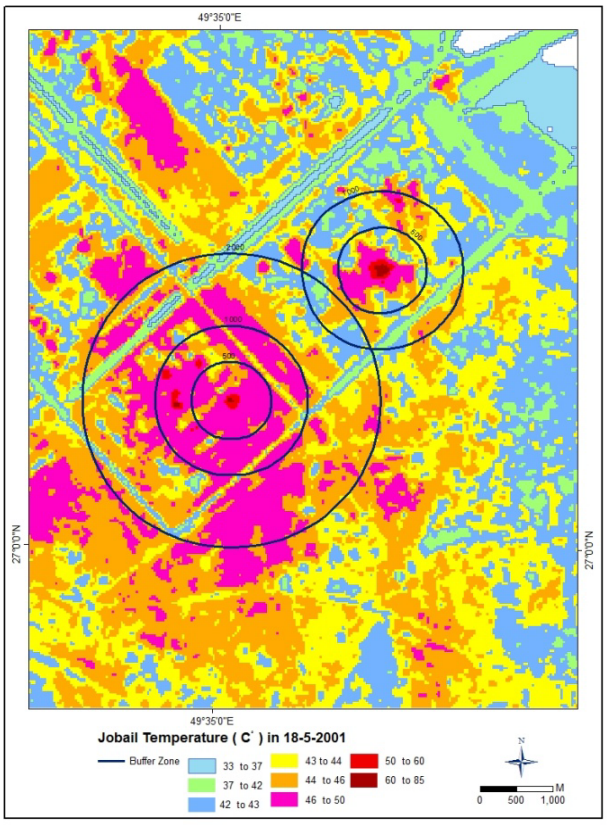

Figure 10: Hot spot buffer zone of iron factories.

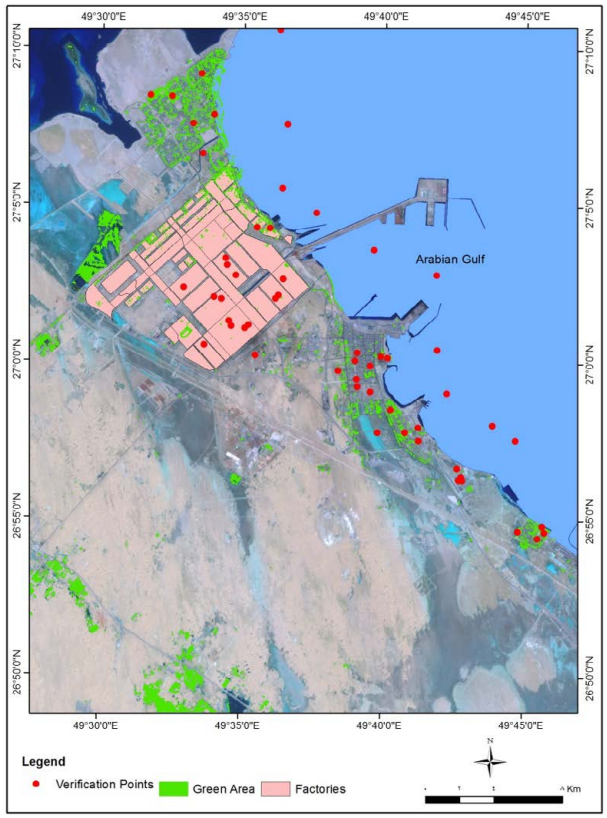

Figure 11: Location of verification point.

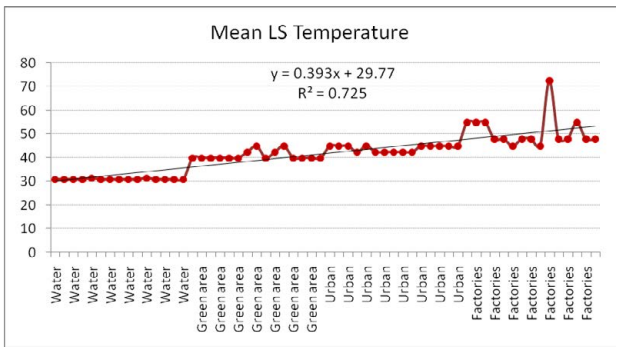

Figure 12: Land surface temperature correlation between land cover.

(Figures 11, 12 and Table 2) which loss of Thermal data, Also, green area helps to decrease temperature depend on density and area size (Figure 10). The amount of vegetation determines LST by the latent heat flux from the surface to atmosphere via evapotranspiration. Lower LST, the planning of green area in valuable for urban climate studies to control of bad impacts.

Conclusions

Surface temperature could be directly derived from remotely sensed data, which provides a powerful way to monitoring urban environment and human activities. This information enhances understanding of urban environment The ETM+ thermal band with 60 m spatial resolution could be used to estimate surface temperature variations and their impact on urban development as well. The surface temperature

ID	Longitude	Latitude	Type	Mean Temp	Max	Min Temp
1	49.60	27.18	Water	31	33	29
2	49.61	27.13	Water	31	33	29
3	49.61	27.09	Water	31	33	29
4	49.63	27.08	Water	31	33	29
5	49.66	27.06	Water	31.5	33	30
6	49.70	27.05	Water	31	33	29
7	49.70	27.01	Water	31	33	29
8	49.70	26.98	Water	31	33	29
9	49.73	26.97	Water	31	33	29
10	49.75	26.96	Water	31	33	29
11	49.82	26.91	Water	31.5	33	30
12	49.86	26.89	Water	31	33	29
13	49.89	26.87	Water	31	33	29
14	49.94	26.87	Water	31	33	29
15	50.01	26.86	Water	31	33	29
16	49.54	27.14	Green area	40	42	38
17	49.53	27.14	Green area	40	42	38
18	49.56	27.15	Green area	40	42	38
19	49.55	27.13	Green area	40	42	38
20	49.57	27.13	Green area	40	42	38
21	49.59	27.07	Green area	40	42	38
22	49.60	27.07	Green area	42.5	43	42
23	49.67	27.00	Green area	45	46	44
24	49.67	27.00	Green area	40	42	38
25	49.67	26.98	Green area	42.5	43	42
26	49.68	26.96	Green area	45	46	44
27	49.69	26.97	Green area	40	42	38
28	49.71	26.94	Green area	40	42	38
29	49.75	26.91	Green area	40	42	38
30	49.76	26.91	Green area	40	42	38
31	49.56	27.11	Urban	45	46	44
32	49.66	27.00	Urban	45	46	44
33	49.65	27.01	Urban	45	46	44
34	49.65	26.99	Urban	42.5	43	42
35	49.65	26.99	Urban	45	46	44
36	49.65	27.00	Urban	42.5	43	42
37	49.66	26.98	Urban	42.5	43	42
38	49.71	26.94	Urban	42.5	43	42
39	49.71	26.94	Urban	42.5	43	42
40	49.71	26.94	Urban	42.5	43	42
41	49.69	26.96	Urban	45	46	44
42	49.76	26.91	Urban	45	46	44
43	49.66	26.96	Urban	45	46	44
44	49.64	27.00	Urban	45	46	44
45	49.76	26.91	Urban	45	46	44
46	49.59	27.02	Factories	55	60	50
47	49.58	27.02	Factories	55	60	50
48	49.58	27.02	Factories	55	60	50
49	49.59	27.02	Factories	48	50	46
50	49.57	27.05	Factories	48	50	46
51	49.58	27.05	Factories	45	46	44
52	49.57	27.03	Factories	48	50	46
53	49.57	27.03	Factories	48	50	46
54	49.55	27.04	Factories	45	46	44
55	49.60	27.04	Factories	72.5	85	60
56	49.60	27.03	Factories	48	50	46
57	49.57	27.06	Factories	48	50	46
58	49.61	27.04	Factories	55	60	50
59	49.59	27.00	Factories	48	50	46
60	49.56	27.01	Factories	48	50	46

Table 2: Location and Value of Land surface temperature in Jubail.

is mainly affected by the land use types; that increased by factories and also decreased by the Green and water land cover. Relationship between urban surface temperature and land cover types enabled us to find out the best solution for urban planning strategies that meet heat island reduction. The integration of remotely sensing data into GIS can be a powerful tool in planning and managing a research work involving spatial data analysis to develop a decision-support system; to build and consulted for proper decisions in the agriculture, grazing and continues development. It is recommended to surround the industrial areas by green belt buffers to more than 500-1500 m for improving temperature condition and to decrease pollution effects to the acceptable limits. This paper will be greatly useful and convenient for those who are studying the ground thermal environment and urban heat island effects by using Landsat ETM+ images.

References

1. Wan Z, Snyder W, Zhang Y (1996) Validation of land surface temperature retrieval from space. Proceedings IGARSS 4: 2095-2097.
2. Roth M, Oke TR, Emery WJ (1989) Satellite-derived urban heat islands from three coastal cities and the utilization of such data in urban climatology. Int J Remote Sens 10: 1699-1720.
3. Serban C, Maftei C Thermal analysis of climate regions using remote sensing and grid computing. International Journal of Computer Networks & Communications 3: 35-51.
4. Ackerman B (1985) Temporal march of the Chicago heat island. Journal of Climate Applied Meteorology 24: 547-554.
5. Setturu B, Rajan KS, Ramachandra TV (2013) Land Surface Temperature Responses to Land Use Land Cover Dynamics. Geoinformatics & Geostatistics: An Overview1: 4.
6. Weng Q (2009) Thermal infrared remote sensing for urban climate and environmental studies: Methods, applications, and trends. ISPRS Journal of Photogrammetry and Remote Sensing 64 (4): 335-344.
7. Quattrochi DA, Luvall JC (1999) Thermal infrared remote sensing for analysis of landscape ecological processes: methods and applications. Landscape Ecology 14 (6): 577-598.
8. Li Y, Zhanga H, Kainz W (2012) Monitoring patterns of urban heat islands of the fast-growing Shanghai metropolis, China: Using time-series of Landsat TM/ETM+ data. International Journal of Applied Earth Observation and Geoinformation 19: 127-138.
9. Rajasekar U, Weng Q (2009) Urban heat island monitoring and analysis using nonparametric model: A case of Indianapolis. ISPRS Journal of Remote Sensing 64: 86-96.
10. Weng Q, Lu D, Schubring J (2004) Estimation of land surface temperature vegetation abundance relationship for urban heat island studies. Remote sensing of Environment 89: 467-483.
11. Saudi Aramco World (1982) Jubail, Saudi Arabia, Foundations: The New Cities, ND 82: 30-40.
12. Saudi Arabia meteorology and environmental protection agency Report 2010.
13. NASA (2009) Landsat 7 Science Data Users Handbook, Chapter 11 pp: 117-120.
14. ENVI version 5.1 (2014) Help, Exelis Visual Information Solutions, Boulder, Colorado.
15. Yale Documentation 2014.
16. USGS, Landsat 7 Science Data User's. Handbook (2001).
17. Barsi JA, Schott JR, Palluconi FD, Hook SJ (2005) Validation of a web-based atmospheric correction tool for single thermal band instruments. Proceedings SPIE 5882: 58820E.
18. Jing J, GuangjinT (2010) Analysis of the impact of Land use/Land cover change on Land Surface Temperature with Remote Sensing. Procedia Environmental Sciences 2: 571-575.
19. Weng Q (2001) A remote sensing - GIS Evaluation of Urban Expansion and Its Impact on Surface temperature in the Zhujiang Delta, China. International journal of remote sensing 22: 1999-2014.
20. Asmat A, Mansor S, Tai Hong W (2003) Rule based classification for Urban Heat Island Mapping. Proceedings of the 2nd FIG Regional Conference Marrakech, Morocco, pp: 1-11.

This article was originally published in a special issue, **Environment: Globalization and Urbanization** handled by Editor. Dr. Raymond J. Dezzani, University of Idaho